THE X-RAY INTENSITY DISTRIBUTION OF THE SOLAR CORONA AND ITS VARIABILITY

H. Hara

Institute of Astronomy, The University of Tokyo
2-21-1 Osawa, Mitaka, Tokyo 181, Japan

Abstract

We report initial analysis of image brightness distributions that concisely represent the spatial structure of the solar X-ray corona. This research makes use of histograms of pixel brightnesses obtained from whole-Sun images from the soft X-ray telescope (SXT) aboard *Yohkoh*. We discover that the soft X-ray intensity histogram essentially consists of a power-law distribution in bright regions and another one in less bright regions. Active regions show a power-law intensity distribution, whereas quiet regions have non-power law distribution. The comparison of the histograms in the active and less active phases shows that the integrated soft X-ray variability is related to a variation of the total area and the appearance/disappearance of bright component of active regions. The overall shapes of the X-ray histograms are similar to those of histograms of the photospheric magnetic fields given by Schrijver and Harvey (1989), implying that a coronal brightness distribution is related to a magnetic field distribution on the photosphere.

1. Introduction

The variability of the solar irradiance and its origin is one of the most interesting topics in the solar physics. Although the total X-ray variability can be investigated by simple photometric data (e.g. GOES), the soft X-ray telescope (SXT, Tsuneta *et al.* 1991) of *Yohkoh* (Ogawara *et al.* 1991) allows us to study in detail the spatial distribution of X-ray brightness and its variability owing to the low scattering mirror and CCD camera. During the first two years of synoptic whole-Sun X-ray imaging, beginning in September 1991, the Sun has been drastically changing its appearance in X-rays as it approaches the cycle minimum.

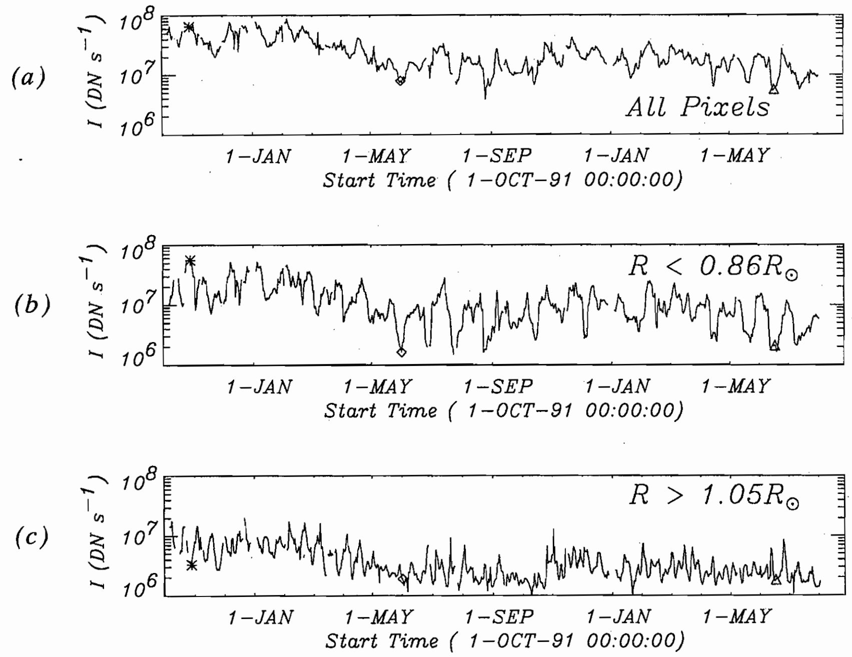

Fig. 1. Temporal variation of the integrated soft X-rays observed by SXT. (a) Integration over the field of view, (b) within 0.86 $R_\odot$, and (c) outside of 1.05 $R_\odot$.

2. Data

The data used in this study are SXT images with thin-Al filter and the pixel size of about $5''$. Composite images are made from two separate exposures with different durations in order to have a wider dynamic range. ¿From the composite images, the intensity histograms $|dN(>I)/dI|$ are created as a function of the X-ray intensity I, where $N(>I)$ is the number of pixels with X-ray intensities larger than I. Three histograms are presented in Figure 2: (1) a histogram for the entire field of view, (2) within 0.86 $R_\odot$, and (3) outside of 1.05 $R_\odot$.

3. Results

Figure 1 shows the temporal variations of the integrated soft X-rays observed by SXT. Minimum X-ray intensities during a day are used in the plot to eliminate the fluctuations due to transient phenomena. The unit of the soft X-ray intensity is DN/s, where 1 DN is equivalent to an energy deposition of approximately 365 eV in the detector. The total X-ray flux (Figure 1-(a)) shows a gradual decrease of the soft X-ray flux from February 1992 to June 1992. The flux begins to increase around September 1992, and then decreases again. In addition to the long term activity, there are variabilities with shorter time scales. Figure 1-(c) shows rapid changes of the soft X-ray flux, faster than the solar rotation period.

Histograms in active (1991 October 29) and less active (1992 June 1) phases marked in Figure 1 are indicated in Figure 2-(a) and 2-(b). We notice that bright components of the histograms disappear in the less active phase of the soft X-ray variability and that the number of pixels in the bright corona decreases compared with the distribution in the active phase. The former may be related to a difference in the occurrence rate of microflares in active regions that appeared at each phase. The latter fact indicates that the total area in active regions become smaller when the solar activity becomes lower. Both distributions essentially have a power-law shape, and the power-law index in the less active phase seems to be slightly steeper

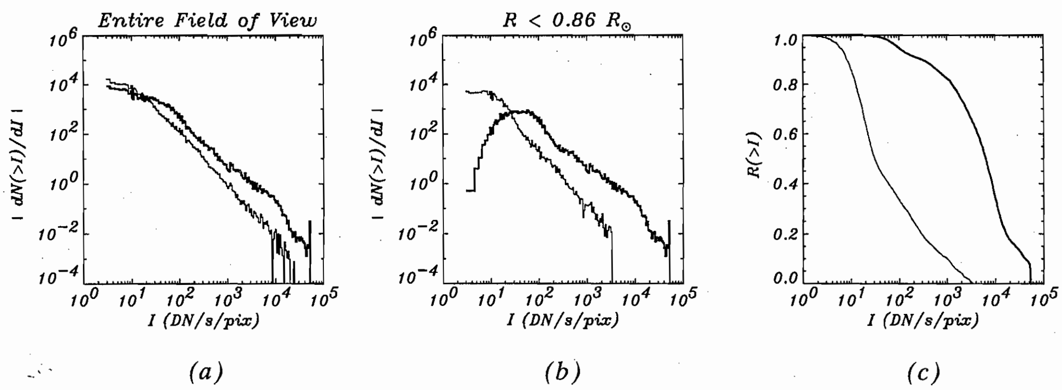

Fig. 2. Soft X-ray histograms for active and less active phases. Thick (thin) line shows the histogram for active (less active) phase on 1991 October 29 (1992 June 1), corresponding to the asterisk (diamond) in Figure 1. (a) Histograms for the entire field of view, (b) those for R $<$ 0.86 $R_\odot$, and (c) the fraction of intensity contribution $R(>I)$.

than in the active phase.

As the solar activity becomes lower than that of 1992 June 1, the total active-region area decreases further, and two distinct distributions appear in the histograms as shown in Figure 3. Figure 3 shows that active regions correspond to a power-law portion in the histogram and that quiet regions have a different intensity distribution, which appears to be well fitted by an exponential law. The threshold intensity level is around 100 DN/s/pixel (1 pixel = $5'' \times 5''$). The distribution of quiet regions seems to be usually hidden by the power-law distributions originating in active regions.

Figure 2-(c) indicates the fraction of intensity contribution $R(>I)$ defined by

$$R(>I) = \frac{\int_I^\infty I' |\frac{dN}{dI'}| dI'}{\int_0^\infty I' |\frac{dN}{dI'}| dI'}$$

for the entire field of view observed by SXT. This figure shows that the contribution from active regions is about 95 percent in the active phase, whereas about 30 percent in the less active phase. It must however be pointed out that the response of SXT is different between active regions and quiet regions because of its temperature dependence.

4. Discussion

Power-law distributions can be also seen in the histograms of the magnetic flux (Schrijver and Harvey 1989), implying that the coronal heating is related to the magnetic field and active-region structures on the photosphere reflect those of coronal regions. When there are two histograms, $|dN/dI| \propto I^{-\alpha}$ and $|\, dN'/d|\phi| \,| \propto |\phi|^{-\beta}$ (ϕ; magnetic flux), I and $|\phi|$ are connected by a power-law relation as $I \propto |\phi|^\gamma (\gamma \equiv (\beta - 1)/(\alpha - 1))$ if N is proportional to N'. If we take $\alpha = 1.6 \sim 2.2$ and $\beta = 1.8 \sim 2.2$ (from Schrijver and Harvey 1989), we obtain $\bar{\gamma} \sim 1$. This is consistent with Saar and Schrijver (1988), but different from Golub et al. (1980). A detailed comparison of the histograms between X-rays and the photospheric magnetic fields is in progress.

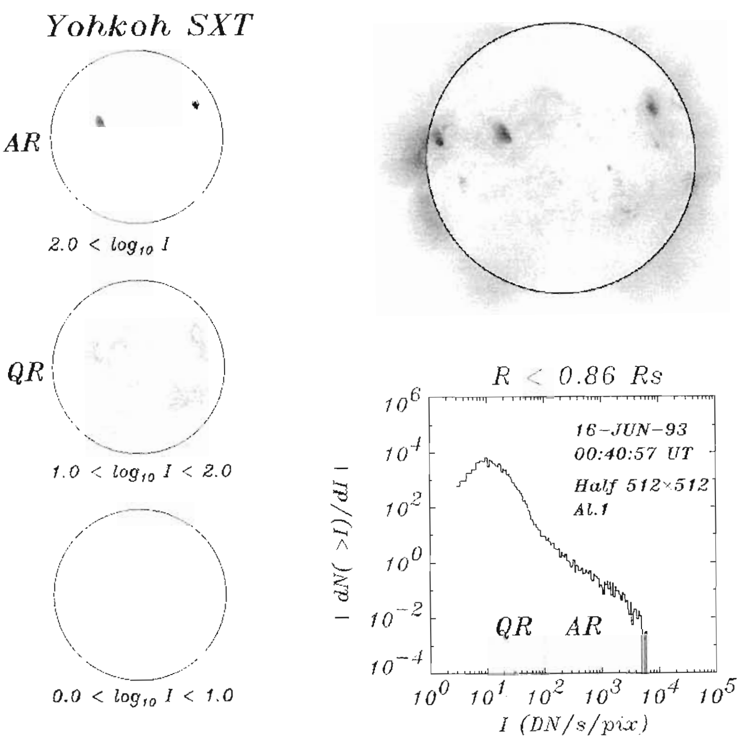

Fig. 3. A soft X-ray histogram (bottom right) on 1993 June 16 (triangle in Figure 1) made from an SXT composite image (top right) within 0.86 $R_\odot$. AR and QR indicate active and quiet regions, respectively. Left figures show the locations which correspond to three portions divided by the intensity thresholds given in the bottom-right figure. Circles in the X-ray images show the limb of the Sun.

The author thanks M. D. Morrison for helping to make the database of X-ray histograms and acknowledges S. Tsuneta and H. S. Hudson for reading the manuscript and giving helpful comments. The author was supported under Fellowships of the Japan Society for the Promotion of Science for Japanese Junior Scientists.

References

1. Golub, L., Maxson, C., Rosner, R., Serio, S., and Vaiana, G. S., 1980, *Astrophys. J.*, **238**, 343.
2. Ogawara, Y., Takano, T., Kato, T., Kosugi, T., Tsuneta, S., Watanabe, T., Kondo, I., and Uchida, Y., 1991, *Solar Phys.*, **136**, 1.
3. Saar, S. H., and Schrijver, C. J., 1988, *Cool Stars, Steller Systems, and the Sun*, eds. J. L. Linsky and R. E. Stencel, Springer, 38.
4. Schrijver, C. J., and Harvey, K. L., 1989, *Astrophys. J.*, **343**, 481.
5. Tsuneta, S., Acton, L., Bruner, M., Lemen, J., Brown, W., Caravalho, R., Catura, R., Freeland, S., Jurcevich, B., Morrison, M., Ogawara, Y., Hirayama, T., and Owens, J., 1991, *Solar Phys.*, **136**, 37.